ELSEVIER

Microporous and Mesoporous Materials 50 (2001) 173–179

MICROPOROUS AND MESOPOROUS MATERIALS

www.elsevier.com/locate/micromeso

The entrapment of UO_2^{2+} in mesoporous MCM-41 and MCM-48 molecular sieves

K. Vidya [a], S.E. Dapurkar [a], P. Selvam [a,*], S.K. Badamali [b], N.M. Gupta [b]

[a] *Department of Chemistry, Indian Institute of Technology – Bombay, Powai, Mumbai 400 076, India*
[b] *Applied Chemistry Division, Bhabha Atomic Research Centre, Trombay, Mumbai 400 085, India*

Received 13 January 2001; received in revised form 14 September 2001; accepted 15 September 2001

Abstract

A method based on direct template-ion-exchange was employed for the entrapment of UO_2^{2+} ions in MCM-41 and MCM-48 molecular sieves via swapping of cetyltrimethylammonium cations present in the mesoporous channels by the UO_2^{2+} ions in an aqueous solution. The samples were characterized by XRD, FT-IR, and ICP-AES techniques. The entrapment of UO_2^{2+} ions is facilitated by the large pore size vis-a-vis the high surfactant content in the as-synthesized host materials. A higher loading of UO_2^{2+} ions was achieved in MCM-48 as compared to MCM-41, which could be attributed to its three-dimensional pore system and higher surfactant-to-silica ratio. FT-IR results provide an evidence of a strong binding of UO_2^{2+} groups with the defect silica sites of mesoporous molecular sieves.

Keywords: Uranyl ions; Mesoporous silica; Ion-exchange; MCM-41; MCM-48

1. Introduction

Over the past few years, porous adsorbent materials have received considerable attention in the recovery of heavy metal ions, e.g., Hg^{2+}, from aqueous wastes, and remain to be a subject of continuing efforts aimed at solving the problems of the environmental clean-up [1]. The selective removal of heavy metal ions or their compounds have become important not only from the point of view of removal of contaminants from wastewater, but also for the recovery of natural resources [2], e.g., extraction of uranium from seawater. A number of adsorbents, viz., montmorillonite clays [3], silica gels [3,4], diatomite (kieselguhr) [5], hydrous oxides [6], etc., have been employed for the sorption of UO_2^{2+} ions from aqueous solution of uranyl salt. However, drawbacks such as small and irregular pore sizes, low surface areas, poor selectivity, low capacity, and inaccessible pores, have limited the possibility of their use to target these toxic metal ions [1].

On the other hand, the discovery [7] of the mesoporous one-dimensional (1D) hexagonal MCM-41 and three-dimensional (3D) cubic MCM-48 silicate molecular sieves, have opened new opportunities in environmental and industrial processes [8]. They have remarkable features such as large surface area (1000–1400 $m^2 g^{-1}$) and uniform pores with well defined and controlled sizes (2–10 nm)

* Corresponding author. Tel.: +91-22-576-7155; fax: +91-22-572-3480/576-7152.
E-mail address: selvam@iitb.ac.in (P. Selvam).

1387-1811/01/$ - see front matter
PII: S1387-1811(01)00445-0

and shapes. These characteristics make the mesoporous materials a prospective candidate for the removal/entrapment of heavy metal ions from aqueous solutions. A number of methodologies, viz., functionalization of mesoporous materials in the removal of mercury [9] and design of selective mesoporous anion traps in the removal of arsenic and chromium in the form of oxyanions [10], have been adopted for this purpose.

In an earlier study, Shin et al. [11] have reported the adsorption of UO_2^{2+} ions on surfactant-free (calcined) mesoporous titanium based materials. These materials are shown to have high capacity for UO_2^{2+} loading compared to the corresponding microporous material. In contrast, in the present study, we used as-synthesized samples of mesoporous materials (MCM-41 and MCM-48) that made the entrapment of the UO_2^{2+} ions feasible through the ion exchange process. The method is based on a direct template-ion-exchange reaction [12–15] between the surfactant cations, i.e., cetyltrimethylammonium ions (CTA^+) in the as-synthesized samples, and the UO_2^{2+} ions in an aqueous system. Experiments were performed both in batch and continuous flow modes. Few comparative tests were also performed on corresponding microporous siliceous samples in order to establish the role of pore structure/size in the UO_2^{2+} sorption process. While the metal loading in the samples was evaluated by inductively coupled plasma-atomic emission spectroscopy (ICP-AES), the nature of host–guest bonding was monitored using Fourier transform infrared spectroscopy (FT-IR). The amount of template leached out during sorption process as a function of time was estimated by total organic content (TOC) or FT-IR method. The effect of uranium loading on crystallinity of the samples was determined using powder X-ray diffraction (XRD) method.

2. Experimental

2.1. Synthesis of mesoporous silicates

The mesoporous MCM-41 and MCM-48 silicate molecular sieves were synthesized hydrothermally [16] as per the procedure described below.

2.1.1. Gel preparation for MCM-41

Tetramethylammonium hydroxide (TMAOH) was diluted with water and stirred for 10 min. To this, fumed silica was added slowly and a homogeneous 'solution-A' was obtained. A 'solution-B' was prepared by mixing cetyltrimethylammonium bromide (CTAB) and NaOH in distilled water, and the solution was stirred for about 30 min. Now, both 'solution-A' and 'solution-B' were mixed together under constant stirring for 1 h. The resulting gel was stirred further for 1 h for homogenization. The typical gel (molar) composition was: SiO_2:0.27 CTAB:0.26 TMAOH:0.26 NaOH:68 H_2O.

2.1.2. Gel preparation for MCM-48

Initially, a 'solution-X' was obtained by mixing NaOH and tetraethyl orthosilicate (TEOS) in distilled water under constant stirring for 10 min. A 'solution-Y' was then prepared by dissolving CTAB in distilled water and was stirred for 20 min. Finally, a homogeneous transparent gel was obtained by mixing the 'solution-X' and 'solution-Y' under constant stirring for 25 min. The resulting gel was stirred further for 1 h for homogenization. The typical gel (molar) composition was: SiO_2:0.6 CTAB:0.5 NaOH:60 H_2O.

2.1.3. Formation of mesoporous silica

Finally, the pH of the gels was adjusted to 11.5 either by adding dilute H_2SO_4 or aqueous NaOH. The gels were placed in an air oven at 373 K for 1 and 3 days for MCM-41 and MCM-48, respectively in Teflon-lined stainless steel autoclaves. The solid products obtained were washed, filtered and dried at 353 K. The resulting samples were designated as as-synthesized MCM-41 and as-synthesized MCM-48, respectively. These samples were then calcined in a tubular furnace at 823 K in a flow of N_2 for 1 or 2 h followed by 8 h in air with a flow rate of 50 ml min^{-1} and a heating rate of 1 K min^{-1}. The samples were designated as calcined MCM-41 and calcined MCM-48 respectively.

2.2. UO_2^{2+} sorption in MCM-41 and MCM-48

2.2.1. Batch mode experiments

To evaluate the efficiency of these mesoporous materials for removal of UO_2^{2+} ions, 1.232 g uranyl

acetate, $UO_2(CH_3COO)_2 \cdot 2H_2O$, was dissolved in 80 ml distilled water (0.035 M) followed by addition of 1 g of as-synthesized MCM-41 or MCM-48. The mixture was stirred at a constant temperature (323 K) and the exchange time varied from 12 to 54 h. It was then washed several times with distilled water and then filtered and dried for 1 h at 353 K. The UO_2^{2+} exchanged MCM-41 and MCM-48 samples were calcined in a tubular furnace at 823 K in a flow of N_2 for 2 h followed by heating in air for 8 h, with a flow rate of 50 ml min^{-1}.

2.2.2. Continuous flow experiments

In these experiments, a 0.035 M aqueous solution of uranyl acetate (~8300 ppm of uranium metal) was passed (0.67 ml min^{-1}) over a bed (2 cm length) of as-synthesized MCM-41, in which about 1 g sample was packed in a glass column plugged with glass wool. The uranium content of the effluent was analyzed periodically by a spectrophotometric method using pyridylazo resorcinol, while the amount of template eluted as a function of time was estimated by TOC.

2.3. Characterization

2.3.1. X-ray diffraction

Power XRD patterns of the ion exchanged and calcined samples were recorded in the 2θ region 1–10° on a Rigaku diffractometer using a nickel filtered CuK_α radiation. The scan speed and step size was 0.2° min^{-1} and 0.02°, respectively.

2.3.2. Thermogravimetry–differential thermal analysis

Thermogravimetry–differential thermal analysis (TG–DTA) measurements were carried out on a Dupont 9900/2100 TG and DTA system in nitrogen atmosphere (50 ml min^{-1}) with 10–15 mg of the sample with heating rate of 10 K min^{-1} in the temperature range of 300–1073 K. The template contents in the as-synthesized MCM-41 and MCM-48 samples were found to be approximately 40% and 50%, respectively.

2.3.3. Surface area and pore size

The surface area was determined by nitrogen adsorption–desorption method using a Sorptomatic at 77 K, which was found to be 848 and 990 ± 20 $m^2 g^{-1}$ for the calcined MCM-41 and MCM-48, respectively. The pore size in both MCM-41 and MCM-48 was found to be in the same range, i.e., 27–30 Å.

2.3.4. Fourier transform infrared

FT-IR spectra of the samples were recorded in mid IR (400–4000 cm^{-1}) region on a Jasco 610 spectrometer at 4 cm^{-1} resolution. Compressed KBr pellets containing 6% sample were used for this purpose. Each spectrum was collected after 100 co-added scans.

2.3.5. Inductively coupled plasma-atomic emission spectroscopy

The amount of uranium loaded in the samples was estimated by ICP-AES, using Labtam Plasma 8440 equipment. A known amount of the calcined sample was placed in a weighed platinum crucible and was dissolved in aqua-regia followed by 40% HF to obtain a clear solution. It was then diluted appropriately with hot water for analysis.

2.3.6. Spectrophotometric determination of uranium

The concentration of uranium in the eluent was determined by a spectrophotometric method [17] using pyridylazo resorcinol in ammoniacal medium, at $\lambda = 530$ nm.

2.3.7. Total organic content

The carbon content in surfactant present in the eluent obtained by continuous flow method was determined by TOC using a Carloerba elemental analyzer 1106.

3. Results and discussion

3.1. Uranium uptake

The uranium loading in the MCM-41 and MCM-48 samples as a function of exchange time with uranyl acetate solution in batch mode experiments is presented in Fig. 1. It can be seen that the uranium loading in MCM-48 reaches saturation in around 20 h and in MCM-41; it reaches saturation in around 25 h of exchange time. It can

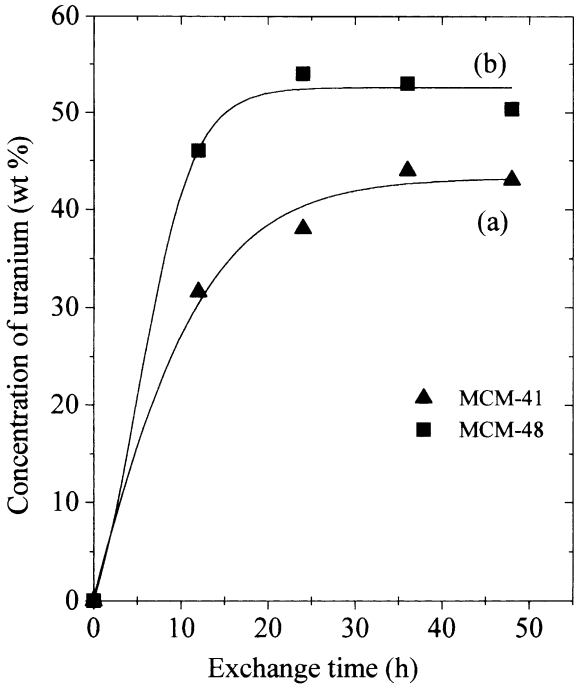

Fig. 1. Uptake of uranium by MCM-41 (a) and MCM-48 (b) in batch mode as a function of exchange time.

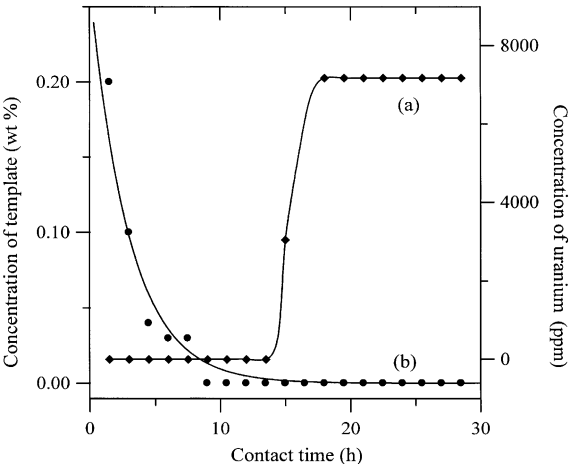

Fig. 2. Concentration of uranium in eluent in continuous flow mode (MCM-41 as fixed bed) (a) and release of template molecules (b) as a function of contact time.

also be seen from the figure that MCM-48 contains ~53 wt.% uranium metal, whereas MCM-41 contains ~43 wt.% uranium metal. When as-synthesized silicalite-1 (surface area 200 $m^2 g^{-1}$; pore size 5.6 Å) was employed under identical experimental conditions, a negligibly small amount of uranium found to be adsorbed (~3.9 wt.%) at the end of 36 h. It is thus evident that the micropores of silicalite-1 restricts the occlusion/diffusion of UO_2^{2+} ions (~4 Å) or corresponding hydrated species (>4 Å). The higher encapsulation capacity of MCM-48 could be correlated with the higher template content in MCM-48 (surfactant/silica = 0.60) as compared to that in MCM-41 (surfactant/silica = 0.27), which could permit an exchange of a larger number of UO_2^{2+} ions. Further, the 3D pore system of MCM-48 and its larger surface area also justifies a larger uranium uptake in this molecular sieve. The data in Fig. 1 also reveals that the time required to reach the equilibrium is apparently shorter in the case of MCM-48 as compared to MCM-41 and is about 1.2 times more than that in MCM-41. This could also be attributed to the 3D pore system in MCM-48, which is capable of higher diffusion of UO_2^{2+} as compared to the 1D pore system in MCM-41.

Fig. 2a represents concentration of uranium in the eluent collected as a function of contact time for as-synthesized MCM-41 in continuous flow experiments. After about 20 h, the concentration of uranium in the eluent reaches a plateau. The concentration of uranium present in the eluent was determined by spectrophotometric method. Thus, the amount of uranium in the mesoporous material was calculated as the difference in the concentrations of uranyl acetate solution before (~8330 ppm) and after contact (~7188 ppm) with MCM-41. This observation was supported by the total amount of uranium uptake by MCM-41, estimated by ICP-AES analysis, which was found to be ~11.5 wt.% or ~1142 ppm. The low uranium uptake by MCM-41 in the continuous flow mode as compared to the batch mode could be attributed to the static and room temperature conditions under which the experiment was carried out. The sorption of UO_2^{2+} ions in the mesoporous MCM-41 occurs by a progressive release of template molecules and a simultaneous saturation of UO_2^{2+} ions. The template removal takes place in 8–9 h, whereas, it takes 14 h for the UO_2^{2+} ions to saturate the column, only after which, the UO_2^{2+} ions start

eluting. If the entrapment of UO_2^{2+} ions occurs predominantly by a template-ion-exchange, then the UO_2^{2+} ions should start eluting immediately after the complete removal of template molecules. However, a time lag of around 4–5 h is observed, which could probably be attributed to the occlusion of UO_2^{2+} ions in the mesopores of MCM-41. Hence, apart from a template-ion-exchange method, occlusion of UO_2^{2+} ions in the mesopores of the molecular sieves could also be considered. The time dependent concentration of template in eluent is evaluated by TOC analysis. Approximately 2.5 ml of eluent was collected every one and a half hours. The samples containing saturation amount of uranium loading (Fig. 1) were employed for detailed characterization, as described below.

3.2. Effect of crystallinity

Shown in Fig. 3 are the powder XRD patterns of as-synthesized MCM-41 and UO_2^{2+} exchanged MCM-41. These data show a strong reflection at $2\theta = \sim 2.11°$ ($d_{100} \sim 41.95$ Å), characteristic of

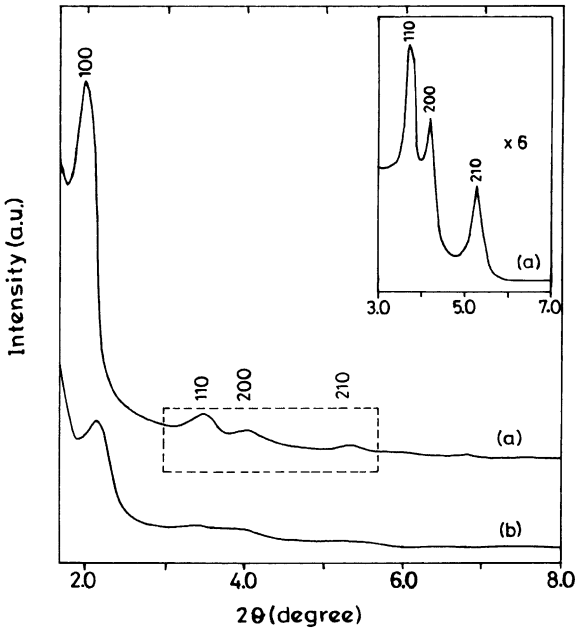

Fig. 3. XRD pattern of as-synthesized MCM-41 (a) and UO_2^{2+} exchanged MCM-41 (b).

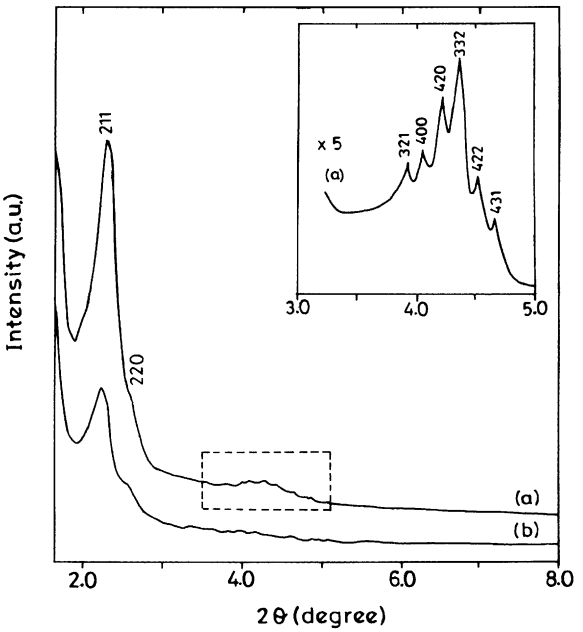

Fig. 4. XRD pattern of as-synthesized MCM-48 (a) and UO_2^{2+} exchanged MCM-48 (b).

hexagonal MCM-41 [7,8,16]. Fig. 4 represents the XRD patterns of as-synthesized MCM-48 and UO_2^{2+} exchanged MCM-48 samples; showing the presence of two major reflections at $2\theta = \sim 2.23°$ ($d_{211} \sim 39.64$ Å) and $2.55°$($d_{220} \sim 34.62$ Å) as well as six minor reflections in the range 3.5°–5.0°, typical of cubic MCM-48 [7,8,16]. XRD data in Figs. 3b and 4b, however, show a broadening and loss of intensity of most of the reflections in the exchanged samples, indicating a partial loss of crystallinity, compared to the host MCM-41 and MCM-48.

3.3. FT-IR results

Fig. 5 depicts the FT-IR spectra of MCM-41 before and after exchanging with uranyl acetate solution for varying periods of time (curves (a)–(d)). The corresponding IR data for MCM-48 sample are given in Fig. 6. The values given in the parentheses in these figures refer to absorbance values of individual bands and are taken as a measure of their relative intensity. The IR bands (ν_{C-H}) at ~2921 and ~2852 cm^{-1} in these spectra

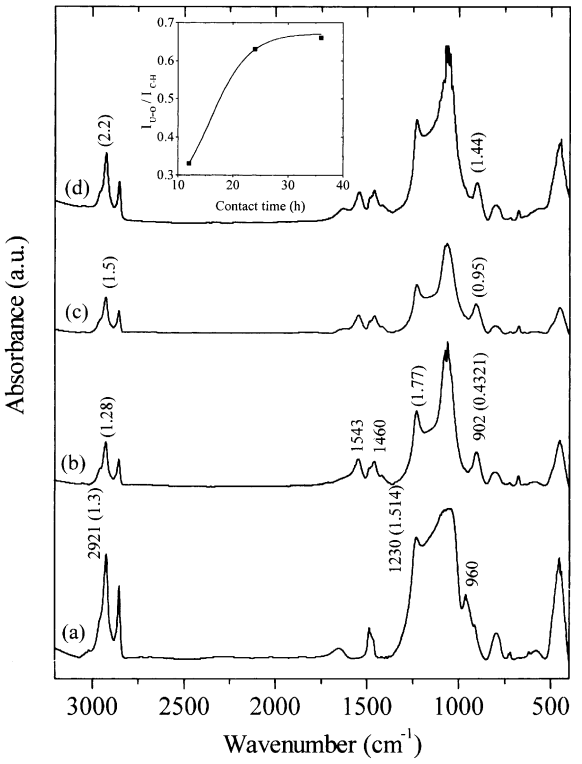

Fig. 5. FT-IR spectra of as-synthesized MCM-41 (a), UO_2^{2+} exchanged MCM-41—12 h (b), UO_2^{2+} exchanged MCM-41—24 h (c), and UO_2^{2+} exchanged MCM-41—36 h (d). The numbers in the parentheses indicate absorbance values. The inset is a plot of ratio of relative intensities of $\nu_{U=O}$ and ν_{C-H} with respect to contact time in MCM-41.

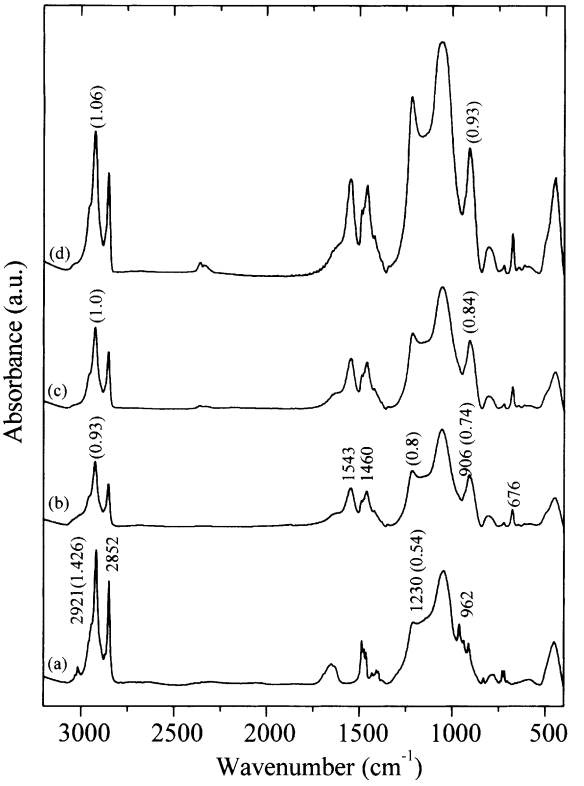

Fig. 6. FT-IR spectra of as-synthesized MCM-48 (a), UO_2^{2+} exchanged MCM-48—12 h (b), UO_2^{2+} exchanged MCM-48—24 h (c), and UO_2^{2+} exchanged MCM-48—36 h (d).

are characteristic of the template molecules, while the bands at ~1230, ~1060 and ~794 cm^{-1} are attributed to the Si–O–Si stretching ($\nu_{Si-O-Si}$) and the bands at ~590, and ~459 cm^{-1} are assigned to Si–O–Si bending ($\delta_{Si-O-Si}$) frequencies of the mesoporous silicate framework [18]. A comparison of these data show the presence of an additional vibrational band at ~902 cm^{-1} in the UO_2^{2+} exchanged MCM-41 and MCM-48 samples (see Figs. 5b, 6b), which may be assigned to asymmetric U=O stretching ($\nu_{U=O}$) of UO_2^{2+} species [19]. The bands appearing at 1543, 1460 (ν_{COO}) and 676 cm^{-1} (δ_{OCO}) are characteristic of the acetate species [19]. The absorbance values given in Fig. 5 clearly reveal the progressive increase in intensity of 902 cm^{-1} band, arising due to UO_2^{2+} species, with increasing loading of uranium. Furthermore, the relative intensities of 902 cm^{-1} ($\nu_{U=O}$) and 2922 cm^{-1} band (ν_{C-H}) increases progressively with the increasing loading of UO_2^{2+} in mesopores (see inset in Fig. 5), and reaches a saturation after 20 h of exchange time. This observation is supported by the uranium uptake in MCM-41 and MCM-48 performed in batch mode and continuous flow experiments. A similar observation was also made in MCM-48 samples. It may thus be inferred that the anchoring of the UO_2^{2+} groups occurs predominantly via a direct replacement of template ions. This inference finds a strong support in the TOC analysis data given in Fig. 2b.

As evaluated from the absorbance values in Figs. 5 and 6, the ratio of A_{902}/A_{1230} in the UO_2^{2+} exchanged samples (12 h) show a higher value for MCM-48 (0.925) than for MCM-41 (0.244), thus indicating a higher UO_2^{2+} content in the former. This observation is also reflected in the ratio of

A_{2921} (exchanged)/A_{2921} (as-synthesized), which shows a lower residual surfactant content in MCM-48 (0.65) than in MCM-41 (0.98), indicating a higher surfactant exchange with UO_2^{2+} species in MCM-48. This observation could be explained by the higher surfactant concentration (molar ratio) in MCM-48 (surfactant/silica = 0.60) than in MCM-41 (surfactant/silica = 0.27) [7,16]. This is supported by the fact that the ratio of absorbance values, A_{2921}/A_{1230}, for as-synthesized samples is higher for MCM-48 (2.66) than for MCM-41 (0.86), as seen in Figs. 5a and 6a. These results thus confirm the important role played by pore structure and high surfactant content in sorption of UO_2^{2+} and are in agreement with the data in Fig. 1, which show a saturation uranium loading of 53 wt.% in MCM-48 compared to about 43 wt.% loading in MCM-41. That is, the uptake of uranium in MCM-48 is about 1.23 times that in MCM-41. This is in good agreement with the amount of template present in MCM-48 (50 wt.%), which is around 1.25 times the template present in MCM-41 (40 wt.%). Hence, we can semi-quantitatively treat the difference in organic contents between MCM-41 and MCM-48 being related to the difference in uranium uptake.

4. Conclusions

In summary, we have demonstrated that the as-synthesized MCM-41 and MCM-48 molecular sieves can be employed for entrapment of UO_2^{2+} species from an aqueous solution. Such an exchange could be accomplished via a direct template-ion-exchange. The UO_2^{2+} groups thus occluded are bonded strongly to defect silica sites in the mesopores of molecular sieves. MCM-48 shows a higher sorption capacity than MCM-41, on account of its high surfactant/silica ratio and three-dimensional pore system.

Acknowledgements

This work is supported by the Board of Research in Nuclear Sciences, Department of Atomic Energy, Mumbai under a contract no. 98/37/31/BRNS/1049. We thank Mr. S. Varma, Applied Chemistry Division, BARC for recording the FT-IR spectra. Our thanks are also due to Mr. E.K. Unnikrishnan, Analytical Chemistry Division, BARC for TOC analysis.

References

[1] L. Mercier, T.J. Pinnavaia, Adv. Mater. 9 (1997) 500.
[2] R.J. Fischer, D. Pang, E. Rosenberg, S. Beathy, Sep. Sci. Tech. 16 (1999) 3125.
[3] J. Dent, J.D.F. Ramsay, S.W. Swaanton, J. Colloid. Interf. Sci. 150 (1992) 45.
[4] P. Michard, E. Guibal, T. Vincent, P. Le Cloirec, Micropor. Mater. 5 (1996) 309.
[5] S. Aytas, S. Akyil, M.A.A. Aslani, U. Aytekin, J. Radioanal. Nucl. Chem. 240 (1999) 973.
[6] A.R. Gupta, B. Venkataramani, Bull. Chem. Soc. Jpn. 61 (1988) 1357.
[7] J.S. Beck, J.C. Vartuli, W.J. Roth, M.E. Leonowicz, K.D. Schmidtt, C.T.-W. Chu, D.H. Olson, E.W. Sheppard, S.B. McCullen, J.B. Higgins, J.L. Schlenker, J. Am. Chem. Soc. 114 (1992) 10834.
[8] P. Selvam, S.K. Bhatia, C. Sonwane, Ind. Eng. Chem. Res. 40 (2001) 3237.
[9] J. Liu, X. Feng, G.E. Fryxell, L.-Q. Wang, A.Y. Kim, M. Gong, Adv. Mater. 10 (1998) 161;
X. Feng, G.E. Fryxell, L.-Q. Wang, A.Y. Kim, J. Liu, K.M. Kemner, Science 276 (1997) 923.
[10] G.E. Fryxell, J. Liu, T.A. Hauser, Z. Nie, K.F. Ferris, S. Mattigod, M. Gong, R.T. Hallen, Chem. Mater. 11 (1999) 2148.
[11] Y.S. Shin, M.C. Burleigh, S. Dai, C.E. Barnes, Z.L. Xue, Radiochim. Acta 84 (1999) 34.
[12] S. Dai, Y. Shin, Y. Ju, M.C. Burleigh, J.-S. Lin, C.E. Barnes, Z. Xue, Adv. Mater. 11 (1999) 1226.
[13] A.-R. Badiei, L. Bonneviot, Inorg. Chem. 37 (1998) 4142.
[14] M. Yonemitsu, Y. Tanaka, M. Iwamoto, Chem. Mater. 9 (1997) 2679.
[15] M. Yonemitsu, Y. Tanaka, M. Iwamoto, J. Catal. 178 (1998) 207.
[16] S.E. Dapurkar, S.K. Badamali, P. Selvam, Catal. Today 68 (2001) 63.
[17] S.C. Chandramouleeswaran, M.B. Sanglikar, S.C. Kumar, M. Sudersanan, in: Proceedings of Symposium NUCAR 2001, Pune, 2001, p. 162.
[18] C.-Y. Chen, H.-X. Li, M.E. Davis, Micropor. Mater. 2 (1993) 17.
[19] K. Nakamoto, Infrared and Raman Spectra of Inorganic and Coordination Compounds, Wiley, New York, 1978.